Dynamics of nitrogen dissociation from direct molecular simulation

Paolo Valentini,[*] Thomas E. Schwartzentruber,[†] Jason D. Bender,[‡] and Graham V. Candler[§]
College of Science and Engineering, Department of Aerospace Engineering and Mechanics, University of Minnesota, Minneapolis, Minnesota 55455, USA
(Received 17 February 2016; published 25 August 2016)

We present a molecular-level investigation of nitrogen dissociation at high temperature. The computational technique, called direct molecular simulation (DMS), solely relies on an *ab initio* potential energy surface and *both* $N_2 + N_2$ and $N + N_2$ processes are simulated as they concurrently take place in an evolving nonequilibrium gas system. Quasiclassical trajectory calculations (QCT) reveal that dissociation rate coefficients calculated at thermal equilibrium, i.e., assuming Boltzmann energy distributions, are approximately equal (within less than 15%) for both $N_2 + N_2$ and $N + N_2$ collisions for the range of temperatures considered. The DMS (nonequilibrium) results indicate, however, that the presence of atomic nitrogen significantly affects the dissociation rate of molecular nitrogen, but indirectly. In fact, the presence of atomic nitrogen causes an important reduction of the vibrational relaxation time of N_2, by almost one order of magnitude. This, in turn, speeds up the replenishment of high-v states that are otherwise significantly depleted if only $N_2 + N_2$ collisions are considered. Because of the strong favoring of dissociation from high-v states, this results in dissociation rates that are 2–3 times higher when significant atomic nitrogen is present compared to systems composed of mainly diatomic nitrogen, such as during the initial onset of dissociation. Specifically, we find that exchange events occur frequently during $N + N_2$ collisions and that such exchange collisions constitute an effective mechanism of scrambling the internal energy states, resulting in multiquantum jumps in vibrational energy levels that effectively promote energy transfers. The resulting vibrational relaxation time constant we calculate for $N + N_2$ collisions is significantly lower than the widely used Millikan-White model. Significant discrepancies are found between predictions of the Park two-temperature model (using the Millikan-White vibrational relaxation model) and the DMS results for dissociating nitrogen systems involving both atomic and molecular nitrogen. Such direct comparisons also illustrate how the DMS method is able to reveal all relevant nonequilibrium physics without the need to compute large numbers of state-transition probabilities. In this manner, DMS presents an accurate and tractable approach to construct models for direct-simulation Monte Carlo and computational fluid dynamics simulations from first principles.

DOI: 10.1103/PhysRevFluids.1.043402

I. INTRODUCTION

Shock layer temperatures at hypersonic conditions often reach many thousands of degrees Kelvin. In this extreme environment, molecular collisions are energetic and cause excitation of internal energy modes, chemical changes in the gas composition, and radiation. Significant coupling between such processes may take place, particularly at very high temperatures. Additionally, because these processes occur over finite time scales that are comparable to characteristic flow times, entire regions of the flow field may be in thermochemical nonequilibrium.

[*]vale0142@umn.edu
[†]schwart@umn.edu
[‡]jbender73@gmail.com
[§]candler@aem.umn.edu

Molecular nitrogen certainly has a key role in how the flow enthalpy is distributed in the internal energy modes of the gas, due to its abundance in Earth's atmosphere. Collisions between nitrogen molecules cause a transfer of energy between the external (translational) and internal (rotational, vibrational, chemical, and electronic) energy modes. In flows characterized by a strong compression of the gas (shock waves), energy is pumped into the upper rovibrational energy levels [1–3] that have been shown to more easily undergo dissociation. Thus, excitation and dissociation resulting from $N_2 + N_2$ collisions are precursors to $N + N_2$ collisions and the formation of NO [2] in air, as well as electronically excited species. Hence, the structure of the shock layer strongly depends on the rates of the dissociation processes and how they are coupled. These physics must be carefully characterized to quantify with accuracy the heat flux that the thermal protection system (TPS) of the vehicle must withstand. This study focuses on the direct molecular simulation of *both* $N_2 + N_2$ *and* $N + N_2$ collisions in the ground electronic state as they concurrently take place in a zero-dimensional evolving gas system. Processes involving $N_2 + N_2$ or $N + N_2$ collisions will be referred to as N_4 or N_3, respectively.

Computational fluid dynamics (CFD) and direct simulation Monte Carlo (DSMC) are methods used to design and size the TPS. Both are macroscopic techniques that require models for the rate of energy transfer between the different molecular degrees of freedom. Current multitemperature thermochemical models [4–7] are formulated to account for preferential dissociation from the upper-level vibrational energy states but are parametrized with experimental measurements obtained at relatively low temperatures. The two-temperature model is most popular and is based on the assumption of a single rotational-translational temperature (i.e., thermal equilibrium between translational and rotational modes), which is different from the vibrational temperature under nonequilibrium conditions. Recent studies [3,8–10], however, have shown a substantial degree of nonequilibrium between rotational and translational modes at temperatures greater than about 15 000 K, thus invalidating the ansatz of a single translational-rotational temperature. In fact, at very high temperatures, relaxation times for rotation and vibration become similar in magnitude and an additional time for internal energy relaxation has been suggested to model the coupled relaxation processes [10]. Under these conditions, a separate rotational temperature should be used, in addition to the vibrational temperature.

Recently, rapid progress in computer technology and computational quantum chemistry methods has enabled research on state-resolved modeling [8,9,11–17]. This approach requires a number of steps. First, a potential energy surface (PES) is constructed: A large set of single-point energy calculations are obtained using a quantum chemistry method. Then, a multidimensional fitting procedure [18,19] is used to fit the energy data. The result is an analytic hypersurface that must be smooth enough to allow evaluation of energy gradients for dynamical calculations (i.e., trajectories). Second, a large number of quasiclassical trajectory calculations (QCT) [20] (or semiclassical calculations [14]) are performed, where the equations of motion are integrated numerically for colliding pairs of molecules. Third, with the use of Monte Carlo sampling techniques, collision cross sections for internal energy transitions and dissociation processes are computed and tabulated [20]. By further integrating over equilibrium velocity distribution functions, energy transition rate coefficients may be obtained as functions of translational temperature. Finally, these rates can be incorporated into master equation analysis, where each quantized rotational-vibrational level is treated as a single species and the full set of species conservation equations are solved with the transition rates incorporated as source terms. In principle, master equation analysis can simulate a chemically reacting nonequilibrium gas without any empiricism and much physical insight can be gained, even from zero-dimensional relaxation simulations [8]. However, a key difficulty with state-resolved approaches is that when all quantized rovibrational states are taken into account, the number of reactions (i.e., transitions between energy levels) is of the order of 10^7 for $N + N_2$ collisions and more than 10^{14} for $N_2 + N_2$ collisions, making full master equation analysis intractable.

Here, we use a different approach, called direct molecular simulation (DMS). The DMS method, also referred to as classical trajectory calculation DSMC (CTC-DSMC), was first proposed by

Matsumoto and Koura [21–23]. It was then extended to rotating and vibrating molecules by Norman, Valentini, and Schwartzentruber [10,24], where the method was also incorporated within a modern parallel DSMC implementation [25]. More recently, Valentini *et al.* [3] have used the DMS method to study nitrogen dissociation using an *ab initio* PES. Unlike standard QCT methodologies, DMS integrates trajectories on a given PES to simulate the gas flow. This results in the direct simulation of an evolving gas system including all relevant physics, for which the only model input is the PES, where all interactions among the various gas species can be, in principle, simulated. In this work, these are diatom-diatom (N_4) and atom-diatom interactions (N_3), of any nature (elastic or not), excluding electronically excited states.

There is no restriction or bias for the energy transitions and dissociation processes that occur during a DMS calculation. Both velocity and internal energy distributions can be arbitrary (nonequilibrium) and evolve depending on the system microstate at a particular time and external constraints (e.g., coupling to a heat bath). Because DMS operates exclusively on atomic positions and velocities (whether bonded in a molecule or not), no *a priori* assumption is made regarding the decoupling of rotational and vibrational energies. In this manner, DMS calculations provide baseline solutions of equal accuracy to full state-resolved DSMC or master equation analyses. As discussed in previous work [3] and this article (Sec. III D), although certain energy transitions (e.g., multiquantum jumps) have a near-zero probability of occurrence, that is generally not known *a priori*. This puts a significant computational burden on state-resolved approaches, which in principle should evaluate cross sections for all possible transitions. In a DMS calculation, however, only the most likely energy transitions actually occur for the conditions of interest [3]. This makes the DMS method feasible for diatom-diatom systems and even polyatomic systems, with modest parallel computing resources [3].

In this work, we extend our previous DMS study [3] to include *both* $N_2 + N_2$ *and* $N + N_2$ collisions on the accurate *ab initio* PES used by Bender *et al.* [26] for their QCT calculations. This PES was obtained by fitting an analytic function to the quantum chemistry data of Paukku and coworkers [18].

The paper is organized as follows: Section II describes the molecular interaction model and the numerical techniques. Section III A contains the results for the vibrational relaxation times for $N + N_2$ and $N_2 + N_2$ inelastic interactions. The results for equilibrium dissociation rates obtained from QCT calculations on N_3 are presented in Sec. III B and compared to the available experimental and computational data. In Sec. III C, nonequilibrium dissociation rates obtained with DMS are presented, with a discussion of the effect of atom-diatom collisions on the overall dissociation process. Section III D contains an analysis of the effect of triatomic exchange events on the dissociation of nitrogen and a comparison with nonreactive transitions under nonequilibrium conditions. A comparison with Park's two-temperature model [6] is detailed in Sec. III E. Lastly, the main conclusions of this study are summarized in Sec. IV.

II. MOLECULAR INTERACTION MODEL AND NUMERICAL METHODS

A. Potential energy surface and trajectory integration

The DMS and QCT approaches used in this article involve the integration of many individual trajectories between pairs of particles. As depicted in Fig. 1, collisions involve either two nitrogen molecules or a nitrogen molecule and a nitrogen atom. While the QCT approach samples pre- and post-trajectory states to obtain average properties of interest, the DMS approach embeds trajectory calculations within a time-accurate flow simulation such that a molecule's or atom's final state after one trajectory becomes its initial state for a future trajectory.

Calculations were conducted using a potential energy surface (PES) that is a global fit to *ab initio* electronic structure data from Paukku *et al.* [18]. This ground-state PES [26], which fits about 17 000 *ab initio* energy data points, describes high-energy rovibrational energy transfers and collision-induced dissociation in $N_2 + N_2$ and $N + N_2$ interactions.

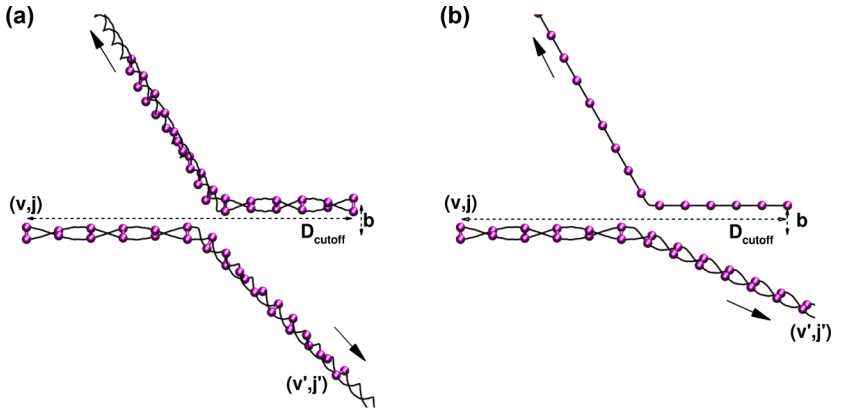

FIG. 1. Schematics of a $N_2 + N_2$ (a) and of a $N + N_2$ (b) trajectory.

As described in a previous article [3], trajectories are initialized with randomized impact parameters and the phase-space coordinates of the nitrogen atoms are numerically propagated in time in order to obtain the post-collision states. The velocity Verlet scheme [27] was used for time integration. The time step is chosen to obtain total energy conservation throughout the trajectory and was set conservatively to 0.05 fs for all simulations presented here. As depicted in Fig. 1, interactions were cut off at $D_{\text{cutoff}} = 15$ Å. To integrate $N + N_2$ trajectories, one of the four atoms (two are bonded in an N_2 molecule) is displaced to a distance much greater than the cutoff D_{cutoff} from the remaining three atoms. This approach is accurate to describe N_3 systems because many first-principles energies corresponding to $N + N_2$ geometries (with a nitrogen atom very far away) [18] were included in the quantum chemistry calculations underlying the PES used in this study.

B. Zero-dimensional system initialization

All zero-dimensional calculations presented in this article are under isothermal conditions. Initial compositions were set with molecular nitrogen partial density $\rho_{N_2}/\rho_{\text{tot}}$ equal to 1. For selected cases, in Secs. III A and III C, $\rho_{N_2}/\rho_{\text{tot}}$ was reduced to 0.01 to isolate N_3 collisions. For systems with $\rho_{N_2}/\rho_{\text{tot}} = 1$ at $t = 0$, $N_p = 1 \times 10^6$ nitrogen molecules were initialized within a volume V at translational temperatures of 20 000 K and 30 000 K. For systems at 10 000 K, instead, 61 440 nitrogen molecules were used. On the other hand, for $\rho_{N_2}/\rho_{\text{tot}} = 0.01$ at $t = 0$, N_p was increased to 8×10^6 for all temperatures in order to obtain satisfactory statistics on the N_2 subset of molecules. In DMS, similarly to standard DSMC, each molecule in the simulation can represent a large number (W_p) of identical molecules, such that the number density is given by $n = N_p W_p / V$. Here, we set ρ_{tot} to 1.2 kg/m^3 and selected V to obtain $W_p = 1$ for all cases. For zero-dimensional simulations, volume V and simulation weight W_p are completely arbitrary. Density only imposes an absolute time scale for the collision rate (see Sec. II C) and, consequently, an absolute time scale seen in the DMS relaxation results.

Particles are initialized in the following manner. Each particle stores the position and velocity vectors of its constituent atoms, either two bonded atoms for N_2 or a single N atom. In the case of molecules, the separation distance between the two atoms is initialized to the equilibrium bond length for nitrogen and the center-of-mass position is randomized within the volume. The velocity vectors of the two atoms *relative* to the center-of-mass velocity are set to achieve a specified vibrational energy (the component parallel to the molecular axis) and rotational energy (the component normal to the molecular axis). A center-of-mass velocity for the molecule is then added to these relative atom velocities. To initialize an isothermal relaxation simulation, center-of-mass velocities are drawn from a Maxwell-Boltzmann distribution at the selected translational temperature, and rovibrational energies are sampled according to Boltzmann distributions at the chosen rotational

and vibrational temperatures. The quasiclassical procedure used to assign rovibrational levels was that of Bender *et al.* [26] using the Wentzel-Brillouin-Kramers method that determines all the allowed quantized rovibrational levels specific to the PES. The above procedure initializes the properties of all nitrogen atoms within a diatomic nitrogen gas system corresponding to a set of initial temperatures $[T_t(0), T_r(0), T_v(0)]$. For atoms, velocities are also simply drawn from a Maxwell-Boltzmann distribution at the selected translational temperature.

C. Collision rate and trajectory initialization

During each DMS time step, a fraction of the particles (both atoms and molecules) in the volume are selected to undergo trajectories corresponding to the collision rate in the gas. The no-time-counter (NTC) method [28], commonly used in DSMC, is employed where the hard-sphere cross section (σ) must be set consistently with the maximum impact parameter ($b_{\max}$) used for the trajectories:

$$\sigma = \pi b_{\max}^2. \tag{1}$$

The DMS algorithm and equations used to select pairs for trajectories is detailed in Ref. [3].

At variance with our previous work [3], we now use the NTC algorithm to select molecule-molecule, molecule-atom, and atom-atom pairs. Trajectories are then integrated for molecule-molecule and molecule-atom pairs as depicted in Fig. 1. For atom-atom pairs, trajectories are not integrated because their velocities (similarly to the center-of-mass velocities of molecules) are sampled from Maxwell-Boltzmann distributions after each Δt_{DMS} to maintain isothermal conditions.

A trajectory calculation for each pair is initialized and performed in a similar manner as the QCT approach and is described in detail in Refs. [3,24,26]. We note that post-trajectory energy states of molecules are not quantized and, except for the initialization ($t = 0$) where internal energies are quantized, DMS molecules maintain continuous energy distributions for both pre- and post-trajectory states.

It is also important to note that as long as $b_{\max}$ is chosen conservatively and is used consistently in the hard-sphere cross-section expression [Eq. (1)] and as the maximum impact parameter for trajectories, the precise value of $b_{\max}$ has no effect on the solution. This is true for any type of collision pairs described by the PES. Therefore, there is no need to select different cross sections for the various gas components, as otherwise necessary in conventional DSMC. The article by Norman and coworkers [24] contains more details on this, and solution independence of the value for $b_{\max}$ was demonstrated in a previous paper [3]. In this work, in light of the results of Bender *et al.* [26], $b_{\max}$ was set conservatively to 6 Å for all simulations.

D. Treatment of dissociation and exchange reactions

After a trajectory is complete, if the two atoms belonging to a molecule are found to be at a distance greater than 6 Å, then the molecule has dissociated. The pre- and post-trajectory states are recorded for postprocessing. At variance with our previous study [3], atoms resulting from a dissociation are not removed from the simulation box and are later randomly selected for collisions with other nitrogen molecules. In this manner, molecular energy transfer and dissociation processes occur due to both $N_2 + N_2$ and $N + N_2$ collisions.

In previous studies based on state-resolved calculations [8,9], exchange processes were found to significantly affect dissociation rates in $N + N_2$ systems. Within the DMS framework, atomic trajectories are simply integrated on the PES given certain initial conditions, and bonds (minima in the free-energy-surface landscape) are created, destroyed, and recreated. Hence, no special treatment is required for any process that can be described by the PES, including exchange reactions. The statistics collected on exchange events, presented in Sec. III D, are obtained only in a postprocessing step.

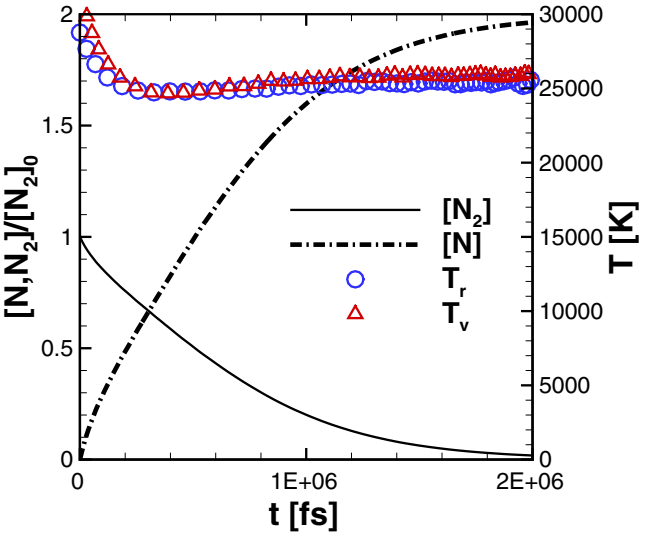

FIG. 2. Example of temperature and composition histories obtained from DMS at $T_t = T_r(0) = T_v(0) = 30\,000$ K.

E. Isothermal relaxation simulations

A DMS relaxation calculation provides the history of integral quantities (e.g., total energies) as well as distributions of external and internal energies. In general, due to translational-internal energy transfer, the instantaneous translational temperature of the system may also change as a function of time (e.g., adiabatic conditions). Once again, to maintain isothermal conditions, we impose a constant translational temperature by re-sampling translational velocities from Maxwell-Boltzmann distributions at the selected T_t for both atoms and molecules after each simulation time step Δt_{DMS}.

Typical results from a simulation are shown in Fig. 2. The system is initialized to $T_t(0) = T_r(0) = T_v(0) = 30\,000$ K. Dissociation of molecular nitrogen is immediate, initially due only to $N_2 + N_2$ collisions, but later also due to $N + N_2$ collisions. Internal energy is rapidly removed from both rotational and vibrational modes (due to dissociation). This leads to a quasisteady state (QSS) characterized by time-invariant nonequilibrium distributions. Because no recombination is modeled, molecular nitrogen keeps dissociating until the system is only comprised of nitrogen atoms, similar to the state-resolved DSMC computations of Kim and Boyd [9].

In the upcoming section, we discuss the internal energy distribution functions during QSS to determine the underlying nonequilibirum physics that couple internal energy exchange and dissociation processes. For example, distributions of external and internal energy modes at $t = 0$ and during steady state, corresponding to the $T_t = 30\,000$ K DMS simulation (Fig. 2), are plotted in Fig. 3. Both molecules and atoms have translational velocities that are distributed according to Maxwell-Boltzmann distributions due to the imposed thermostat. Unlike the translational mode, rotational and vibrational modes are not constrained to equilibrium distributions. Due to dissociation, internal energy distributions change drastically from the initial (quantized) Boltzmann distributions to continuous distributions in QSS, markedly characterized by a significant depletion of high-energy states [Fig. 3(d)], as discussed at length in our previous work [3].

III. RESULTS

A. Vibrational relaxation time for atom-diatom collisions

Vibrational relaxation and chemical dissociation are strongly coupled processes. Upper-level vibrational states are more likely to dissociate and, thus, their populations become depleted [3].

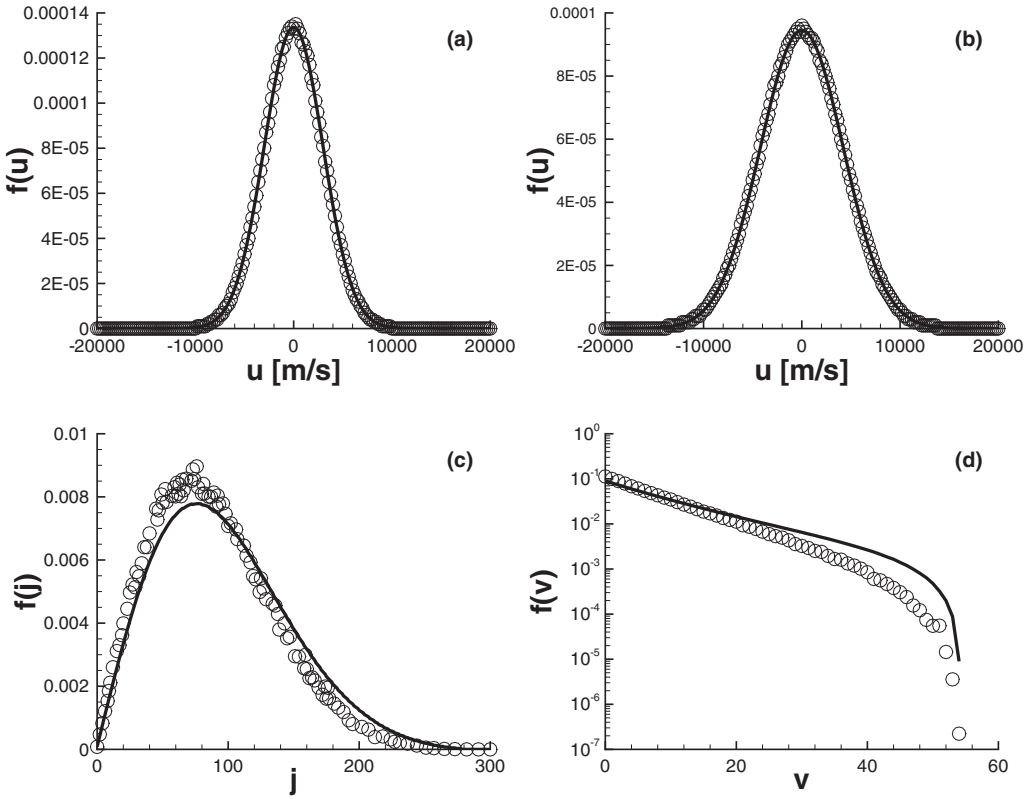

FIG. 3. QSS distributions (circles) from DMS at $T_t = 30\,000$ K: (a) molecular translational velocity distribution, (b) atomic translational velocity distribution, (c) rotational, and (d) vibrational distributions. Solid lines indicate the initial equilibrium distributions.

Vibrational excitation is the mechanism that repopulates the high-v states at the distribution tail. Under nonequilibrium conditions, because of the strong bias of dissociation from high-v states and the finite time to repopulate such states, dissociation proceeds at a rate 4–5 times slower than under equilibrium conditions at the corresponding translational temperature. Remarkably, we found that even a slight depletion of high-energy tails affects the dissociation rates by a significant factor ($\sim$4 to 5) [3].

For $N_2 + N_2$ only systems [3], our PES was shown to predict vibrational relaxation times in close agreement with the Millikan-White correlation and its high-temperature corrections [5,29,30] in the temperature range of 6 000 to 30 000 K. For $N + N_2$ collisions, however, previous QCT-based studies [8,9], utilizing an *ab initio* PES as well, have shown that vibrational relaxation of molecular nitrogen due to collisions with nitrogen atoms proceeds at a rate about an order of magnitude faster than for the diatom-diatom collision case.

In DMS, at each time step, thousands of collisions occur between pairs of molecules or pairs of atoms and molecules, depending on the instantaneous microstate of the system. Hence, to isolate the influence of $N + N_2$ collisions on the vibrational relaxation process, simulations were repeated by reducing the partial density $\rho_{N_2}/\rho_{\text{tot}}$ of N_2 in the box, where ρ_{tot} denotes the total mass density. Vibrational relaxation times were obtained, using the e-folding method [8,31] (i.e., the time required by the energy mode to reach 63.2% of its steady-state energy), by fitting the internal energy histories obtained from the DMS simulations using the Landau-Teller relaxation equation for a classical system. The simulation parameters were set conservatively to $dt = 0.05$ fs, $D_{\text{cutoff}} = 15$ Å, and $b_{\max} = 6$ Å. The initial nonequilibrium was imposed by setting $T_r(0) = T_v(0) = 3\,000$ K. At

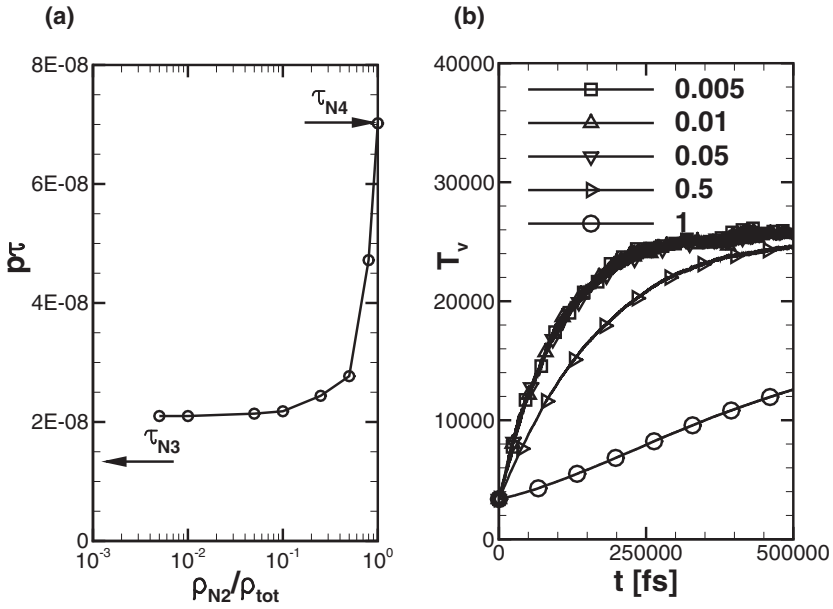

FIG. 4. (a) Characteristic vibrational relaxation times as a function of partial density of molecular nitrogen. (b) Vibrational temperature relaxation histories at various partial densities of molecular nitrogen. Both panels (a) and (b) are for a system at $T_t = 30\,000$ K and $T_r(0) = T_v(0) = 3\,000$ K.

10 000 K, internal energy modes equilibrate with translation before any significant dissociation occurs. However, at 20 000 and 30 000 K, molecules immediately start dissociating, and the relaxation of internal energy is strongly coupled to the dissociation process.

As ρ_{N_2}/ρ_{tot} is reduced, nitrogen molecules are increasingly more likely to collide only with other nitrogen atoms. It is expected that, in the limit of $\rho_{N_2}/\rho_{tot} \to 0$, the obtained vibrational relaxation time $\tau \to \tau_{N_3}$, where τ_{N_3} is due only to $N + N_2$ collisions. The pressure p is the total pressure, namely $pV = N_{N+N_2} k_B T$, where N_{N+N_2} is the total number of particles in the box. As demonstrated in Fig. 4, when ρ_{N_2}/ρ_{tot} is reduced, $p\tau$ reaches a plateau below $\rho_{N_2}/\rho_{tot} = 0.1$. Hence, the simulations to determine τ_{N_3} at the remaining temperatures of 6 000, 10 000, and 20 000 K were conducted at a partial density of 0.01.

Figure 5 summarizes the results for τ_{N_3} for the four temperature cases considered here. In agreement with earlier studies [8,9] using a different PES, computed specifically for the N_3 system, our results show that τ_{N_3} is nearly an order of magnitude smaller than the corresponding characteristic vibrational relaxation time τ_{N_4}. For N_4, our *ab initio* results were found to be in good accordance with Millikan-White correlation (and its high-temperature corrections) [3]. Finally, we note that the Millikan-White correlation, which is written as [29]

$$p\tau = \exp[A(T^{-1/3} - 0.015\mu^{1/4}) - 18.42] \text{ atm s}, \tag{2}$$

where $A = 1.16^{-3}\mu^{1/2}\theta_v^{4/3}$ (θ_v is the characteristic vibrational temperature) contains the reduced mass μ for the colliding pair. By using the appropriate μ for N_3, Eq. (2) predicts only a slight variation of τ_{N_3} compared to τ_{N_4}, thus failing to describe these key physics.

B. $N + N_2$ equilibrium dissociation rates obtained with QCT calculations

High-energy $N + N_2$ collisions were simulated using the QCT method [20,32], similar to our previous study [26] on $N_2 + N_2$ collisions. QCT yields rate constants, given precisely-defined equilibrium thermal distributions of reactants. For this study, at a given temperature T_t, we assume a

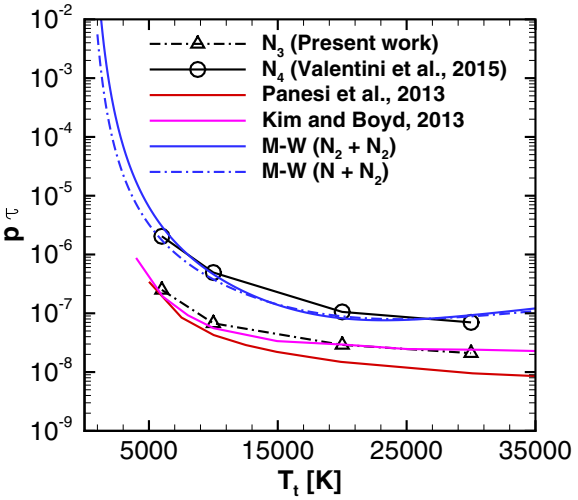

FIG. 5. Vibrational relaxation times obtained from DMS isothermal relaxation simulations for $N + N_2$ collisions ($\rho_{N_2}/\rho_{tot} = 0.01$): comparison to the Millikan-White experimental correlation [29] and high-temperature corrections [5,30], N_4 data from DMS calculations [3], and state-resolved master equation calculations [8] and DSMC calculations [9].

Maxwell-Boltzmann distribution for the relative translational kinetic energy E_r between the N_2 and N reactants and a Boltzmann distribution for the internal energy of N_2. Within this framework, the dissociation rate constant is given by

$$k_{d,N_3}^{QCT}(T_t) = \pi b_{max}^2 \left(\frac{8k_B T_t}{\pi\mu}\right)^{1/2} \int_0^\infty \int_0^{b_{max}} \bar{\bar{\mathscr{P}}}^{(d)}(E_r,b) \left(\frac{2\,b}{b_{max}^2}\right) \Lambda_r \exp(-\Lambda_r) db\, d\Lambda_r. \quad (3)$$

Here, μ is the reduced mass for the two reactants, k_B is the Boltzmann constant, and $\Lambda_r \equiv E_r/k_B T_t$. As in DMS, b is the impact parameter, and b_{max} is the value of b beyond which there is a negligible probability of dissociation. Finally, $\bar{\bar{\mathscr{P}}}^{(d)}(E_r,b)$ is the probability of dissociation averaged over the vibrational and rotational quantum numbers of the reactant N_2 molecule and also over all other parameters (apart from E_r and b) that are needed to specify trajectory initial conditions. A detailed discussion of these concepts and how they are applied can be found in our previous work [26].

Cases were run for $T = 10\,000$ K (24 million trajectories), 20 000 K (9 million trajectories), and 30 000 K (6 million trajectories). In each case, we used stratified sampling on the impact parameter b and a maximum value $b_{max} = 6$ Å. Trajectory motion was computed using a Verlet integrator [27] with a time step $\Delta t = 0.05$ fs. For the purposes of terminating a dissociating trajectory, a molecular bond was considered broken if it exceeded 10 Å.

The results obtained from the QCT calculations are shown in Fig. 6, where they are compared to our previous results for $N_2 + N_2$ [26] and rates inferred from various experimental data (and their extrapolations) for $N + N_2$ [33–36]. In the highlighted experimental range, the QCT results are quite close to the inferred rates of Appleton *et al.* [35] and Cary [34], but differ by almost an order of magnitude from those of Byron [33] and Hanson and Baganoff [36]. The spread in the experimentally inferred rates is quite significant and is about an order of magnitude.

As illustrated in Fig. 6, the comparison with our previous QCT calculations for $N_2 + N_2$ dissociation, obtained from the same PES used in this study, reveals that, under equilibrium conditions, k_{d,N_3}^{QCT} is approximately equal to $k_{d,N_4}^{QCT} = k_d^{QCT}$ (within less than about 15% over the whole temperature range). Therefore, on a per-collision basis, a nitrogen molecule is nearly as effective as a nitrogen atom at dissociating another nitrogen molecule.

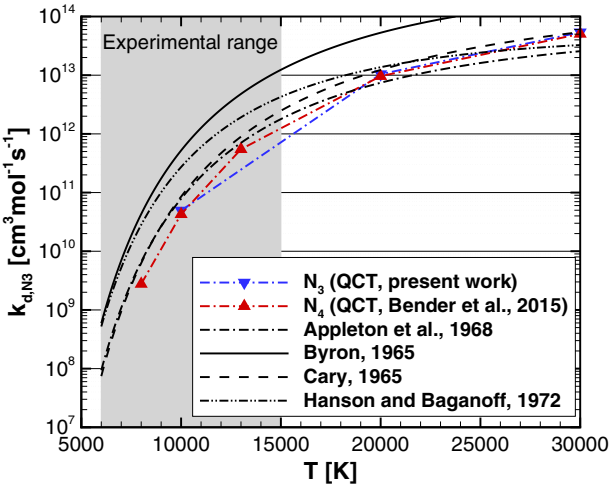

FIG. 6. Comparison between QCT dissociation rate coefficients for $N + N_2$ (present work) and $N_2 + N_2$ [26], and several experimental results with high-temperature extrapolations [33–36].

C. Nonequilibrium dissociation rates

The DMS method was used to characterize the nonequilibrium dissociation process for systems initialized in thermal equilibrium [$T_r(0) = T_v(0) = T_t$]. We considered two chemical compositions to initialize the system and determine k_{d,N_3}^{DMS} using the appropriate reaction rate law.

To begin, simulations were conducted at an initial partial density $\rho_{N_2}/\rho_{tot} = 0.01$. Under these dilute conditions, the vast majority of collisions are between a nitrogen molecule and a nitrogen atom, as discussed in Sec. III A. For the three translational temperatures considered here (10 000, 20 000, and 30 000 K), 8 million particles were used. Total density was set to about 1.2 kg/m^3 and particle weight was set to unity. For this case, the reaction rate law

$$\frac{d[N_2]}{dt} = -k_{d,N_4}^{DMS}[N_2]^2 - k_{d,N_3}^{DMS}[N][N_2] \tag{4}$$

can be simplified to

$$\frac{d[N_2]}{dt} = -k_{d,N_3}^{DMS}[N][N_2], \tag{5}$$

where [ ] denotes molar concentrations in mol/m^3. Furthermore, because $[N](t = 0) \gg [N_2]$, the concentration of nitrogen atoms can be taken as approximately constant with respect to time, i.e., $[N](t) \simeq [N](t = 0) = [N]_0$. Therefore, Eq. (5) can be easily integrated analytically with respect to time t to yield:

$$[N_2](t) = [N_2]_0 \exp\left(-k_{d,N_3}^{DMS}[N]_0 t\right), \tag{6}$$

which is a simple exponential decay of $[N_2](t)$. Equation (6) was then used to fit the QSS portion of the relaxation, when energy distributions remain time invariant. Figure 7(a) shows the DMS simulation result along with the fit that is used to obtain the value of k_{d,N_3}^{DMS}.

As discussed in Sec. III B, QCT calculations showed that $k_{d,N_3}^{QCT} \simeq k_{d,N_4}^{QCT}$, and, therefore, a nitrogen molecule is nearly as effective as a nitrogen atom at dissociating another nitrogen molecule, on a per-collision basis. For this reason, it is reasonable to expect that $k_{d,N_3+N_4}^{DMS} = k_{d,N_3}^{DMS}$. Here, the subscript $N_3 + N_4$ refers to the rate of N_2 dissociation due to collisions with *either* N or N_2. Furthermore, it is important to note that any difference between k_d^{QCT} ($=k_{d,N_3}^{QCT} \simeq k_{d,N_4}^{QCT}$) and $k_{d,N_3+N_4}^{DMS}$ is only a result of the QSS non-Boltzmann vibrational energy distributions found with DMS calculations [as shown in Fig. 3(d)]. Since, in QSS, the tails of the DMS vibrational energy distributions are depleted, we

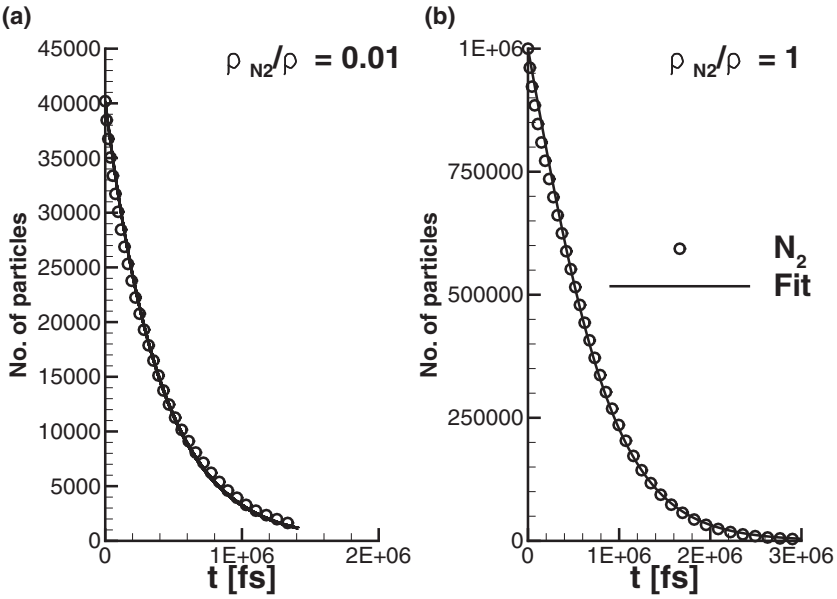

FIG. 7. Number of nitrogen molecules as a function of time from DMS for (a) $\rho_{N_2}/\rho_{tot} = 0.01$ and (b) $\rho_{N_2}/\rho_{tot} = 1$ for a system initially in thermal equilibrium $T_t = T_r(0) = T_v(0) = 30\,000$ K.

expect $k^{DMS}_{d,N_3+N_4} < k^{QCT}_d$. We now quantify these statements through DMS calculations that include significant amounts of both molecular and atomic nitrogen.

Systems were initialized with $\rho_{N_2}/\rho_{tot} = 1$, i.e., comprised of only nitrogen molecules at the initial time. In this case, both $N_2 + N_2$ and $N + N_2$ collisions concurrently take place in the system. The reaction rate law used to fit composition histories in the QSS (when both atomic and molecular nitrogen is present) is, therefore, Eq. (4), which is now written as

$$\frac{d[N_2]}{dt} = -k^{DMS}_{d,N_3+N_4}[N_2]^2 - k^{DMS}_{d,N_3+N_4}[N][N_2]. \tag{7}$$

Figure 7(b) shows the DMS simulation result at 30 000 K for $\rho_{N_2}/\rho_{tot} = 1$, together with the result obtained by integrating Eq. (7) using k^{DMS}_{d,N_3+N_4} ($=k^{DMS}_{d,N_3}$) shown in Fig. 7(a). Hence, a single rate constant $[k^{DMS}_{d,N_3+N_4}(T_t)]$ reproduces DMS results for a system with only N_3 interactions *and* a system with both N_3 and N_4 interactions.

DMS calculations were repeated at $T_t = 10\,000$ K, $T_t = 20\,000$ K, and $T_t = 30\,000$ K with $\rho_{N_2}/\rho_{tot} = 1$ at $t = 0$. The N_2 concentration histories were then fit using Eq. (7) to obtain the value of k^{DMS}_{d,N_3+N_4} at each translational temperature. The results are shown in Fig. 8. Previous data from Valentini *et al.* [3], that only accounted for diatom-diatom collisions (k^{DMS}_{d,N_4}), are also included for comparison. Specifically, the previous results for k^{DMS}_{d,N_4} had been obtained from DMS calculations with systems that only comprised N_2 molecules (atoms produced by dissociation events were immediately removed from the simulation so that $\rho_{N_2}/\rho_{tot} = 1$ at all times). As seen in Fig. 8, the dissociation rate k^{DMS}_{d,N_3+N_4} is roughly 2–3 times larger than the dissociation rate k^{DMS}_{d,N_4}.

The results in Fig. 8 can thus be summarized as follows: $k^{DMS}_{d,N_4} < k^{DMS}_{d,N_3+N_4} < k^{QCT}_{d,N_3} \simeq k^{QCT}_{d,N_4}$. In other words, on a per-collision basis, QCT analysis shows that N_2 and N are nearly equally effective at dissociating a nitrogen molecule. However, the nonequilibrium (QSS) dissociation rates (k^{DMS}_{d,N_4}), obtained from DMS, are 4 to 5 times lower than the corresponding equilibrium values, due to high-v states depletion. Furthermore, in systems characterized by a substantial presence of atomic

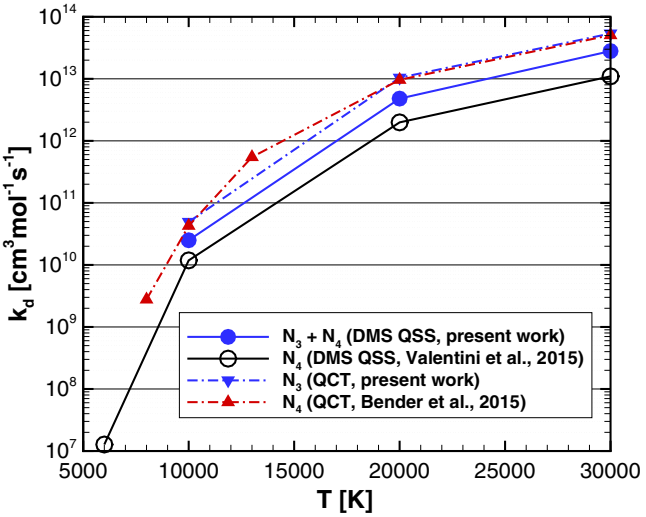

FIG. 8. Comparison between QCT (equilibrium) and DMS dissociation rate coefficients for $N + N_2$ (present work) and $N_2 + N_2$ only [3,26], all based on the same *ab initio* PES [26].

nitrogen, nonequilibrium rates ($k_{d,N_3+N_4}^{DMS}$) are about 2 to 3 times higher than systems that only contain molecular nitrogen.

This physical difference can be explained by analyzing the vibrational energy distributions for the reactants, $f(v)$, that is shown in Figs. 9(a)–9(c). Significant depletion of high-v states is observed, with similar trends with increasing T_t as in N_4 systems [3]. However, collisions with nitrogen atoms reduce the degree of depletion of the high-vibrational-energy populations. In fact, two processes occur simultaneously under nonequilibrium dissociating conditions [3]: (i) removal of energy from

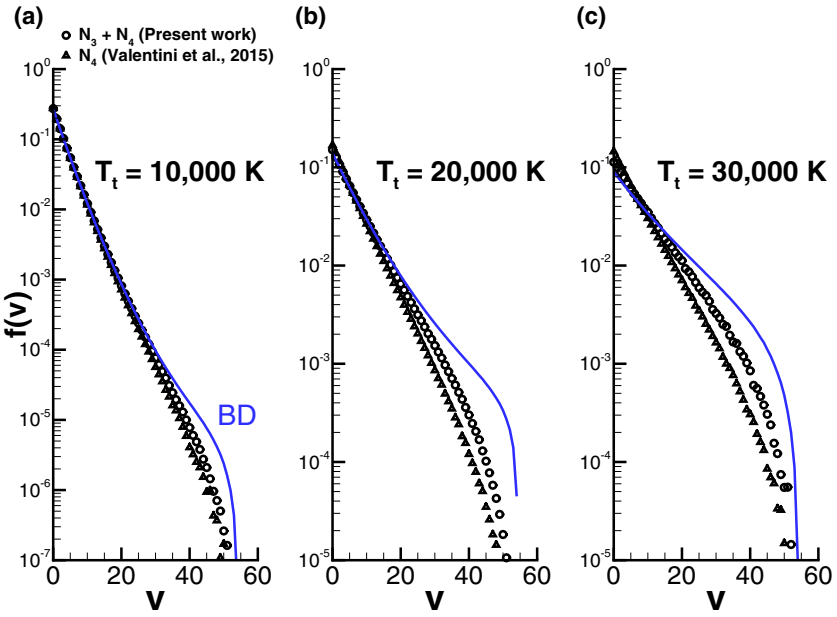

FIG. 9. Vibrational distribution functions for bound states at (a) 10 000, (b) 20 000, and (c) 30 000 K. The data from Valentini *et al.* [3] account for $N_2 + N_2$ processes only. BD denotes the Boltzmann distribution at T_t.

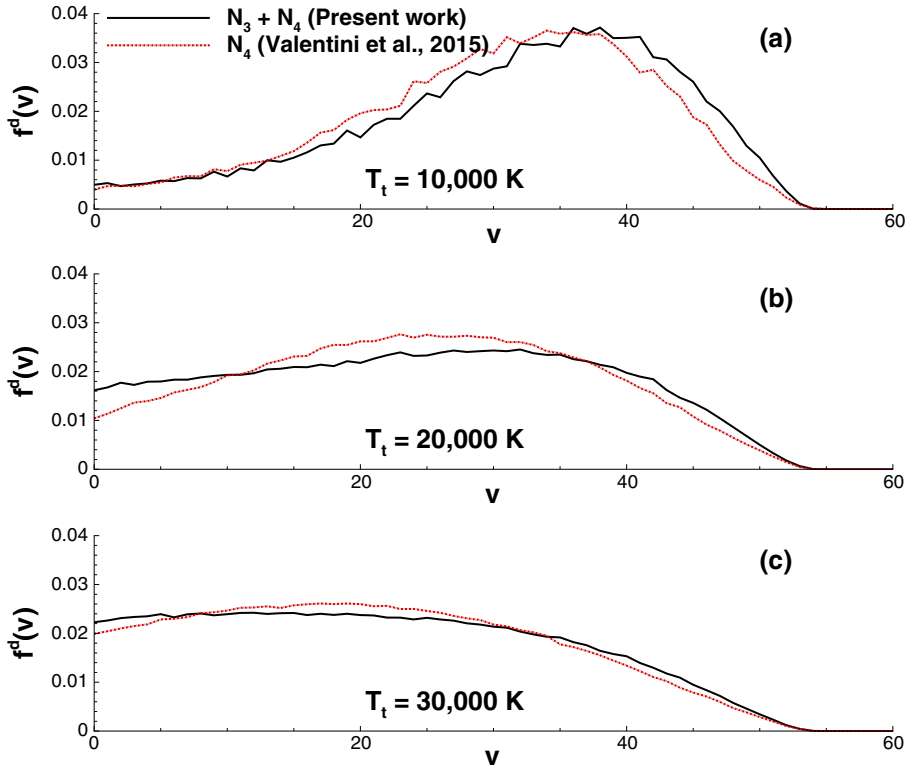

FIG. 10. Vibrational distribution functions for precollision states of dissociated molecules at (a) 10 000, (b) 20 000, and (c) 30 000 K. The data from Valentini *et al.* [3] are relative to $N_2 + N_2$ processes only.

the vibrational manifold due to depletion of high-v states and (ii) replenishment of those same high-v states due to rovibrational excitation from low-v states. Collisions with nitrogen atoms excite molecules vibrationally, on average, more rapidly than collisions with other nitrogen molecules, as indicated by a reduction of almost one order of magnitude in the vibrational relaxation time τ for N_3 compared to N_4 systems (Fig. 5). High-vibrational-energy states, now repopulated at a faster rate, are more likely to dissociate [3]. In turn, this results in a faster dissociation rate than in N_4 systems. Although the change in the distributions [Figs. 10(a)–10(c)] appears relatively small, we found that modest variations in the distribution functions of the molecular reactants produce strong variations in the overall dissociation rate [3], particularly at low temperature (10 000 K), where there is a very strong bias to dissociate from high-v states.

In contrast, previous research [3,26] found that the rotational favoring factor, for high-rotational-energy molecules to dissociate, is much less significant than for high-vibrational-energy molecules. The DMS method simulates both rotational and vibrational excitation including the evolution of non-Boltzmann internal energy distributions. However, similar to our previous research [3], we find that rotational favoring for dissociation, now including N-N_2 collisions, remains significantly less important than the vibrational favoring. For this reason, the current article focuses only on vibrational energy relaxation and coupling to dissociation. Future postprocessing of DMS results could be performed to precisely quantify the influence of rotation, especially in the immediate postshock region where the translational and rotational energies may be much higher than the vibrational energy. In fact, previous QCT [26] and master equation [8] studies show that, in dissociating trajectories where products are in low-vibrational-energy states, rotational energy has to compensate.

The analysis of normalized vibrational energy distributions of dissociated N_2 populations provides important insights into the mechanisms of nonequilibrium dissociation. Figure 10 contains the

TABLE I. Results for exchange processes in N_3 systems from QCT calculations.

T [K]	$k_{ex}^{\mathrm{QCT}}/k_d^{\mathrm{QCT}}$
10 000	252.
20 000	10.7
30 000	4.04

precollision vibrational energy distributions [denoted with $f^d(v)$] of dissociated reactants (i.e., of those N_2 molecules that dissociate in a collision with either another molecule or an atom). Additionally, we compare f^d obtained here with those by Valentini *et al.* [3], which only accounted for diatom-diatom interactions. Exchange processes between two molecules that resulted in a dissociation were excluded from the count of the events because they involve *both* reactant particles, as pointed out by Bender *et al.* [26].

Like we saw in our previous results [3], the precollision vibrational distribution of dissociated molecules $f^d(v)$ is clearly non-Boltzmann and becomes progressively flatter as T_t is increased. At 10 000 K, Fig. 10(a), the majority of molecules that dissociate initially have a vibrational quantum number of about 35 and relatively few have a low vibrational quantum number. As T_t is increased [Figs. 10(b)–10(c)], there is a greater relative contribution to dissociation from low vibrational states due to the increased availability of collision energy from translation. A rapid drop for $f^d(v)$ is then seen at vibrational states near the maximum allowed vibrational quantum number, due to their scarcity in the underlying pool of bound molecules. The temperature-dependent depletion of the mid- to high-energy states is a defining characteristic of nonequilibrium dissociation [3].

D. Exchange reactions

Exchange events are quite rare for $N_2 + N_2$ only systems (up to 6.5% of the dissociation events at 30 000 K [26]). However, we found them to be relatively frequent in $N + N_2$ collisions. As listed in Table I, statistics on triatomic exchange events ($N + N_2$), collected from QCT calculations, show that the exchange reaction rate k_{ex}^{QCT} is strongly influenced by T_t and varies between about $252k_d^{\mathrm{QCT}}$ at 10 000 K and $4k_d^{\mathrm{QCT}}$ at 30 000 K. Figure 11 compares exchange reaction rates for $N + N_2 \rightarrow N_2 + N$ obtained with QCT on the potential energy surface used here and similar QCT data of Esposito and Capitelli [13] based on a different PES. The agreement between the two sets of results is well within an order of magnitude.

Finally, Fig. 12 shows the probability distribution functions for exchange processes from DMS calculations (i.e., for nonequilibrium dissociating conditions) at the three temperatures considered in this study. In Figs. 12(a1)–12(c1), $p(v_i, v_f)$ represents the probability of the exchange reaction characterized by $N + N_2(v_i) \rightarrow N_2(v_f) + N$. Selected *cuts* of $p(v_i, v_f)$ are also shown in Figs. 12(a2)–12(c2). Although rather peaked around v_i, the distributions $p(\{0,10,20,30,40\}, v_f)$ appear quite *diffuse* and asymmetrical around v_i, thus indicating an effective mechanism of scrambling the internal energy states.

The greater likelihood in $N + N_2$ exchange reactions, when compared to nonreactive inelastic collisions, of transitions to high-v states via multiquantum jumps accelerates the vibrational excitation of low-vibrational-energy molecules and results in a smaller relaxation time, i.e., $\tau_{N_3} < \tau_{N_4}$. Such transitions replenish the populations of high-v molecules, which are more likely to dissociate.

To demonstrate the internal energy scrambling effect of exchange reactions, we obtained a probability map for nonreactive $N + N_2$ collisions at 10 000 K, similar to that shown in Fig. 12(a1). As illustrated in Figs. 13(a)–13(b), $p(v_i, v_f)$ for nonreactive collisions is markedly peaked around v_i, in contrast with the corresponding plot for exchange processes. In other words, in quasielastic and inelastic collisions that do not involve a bond breakage, the probability of

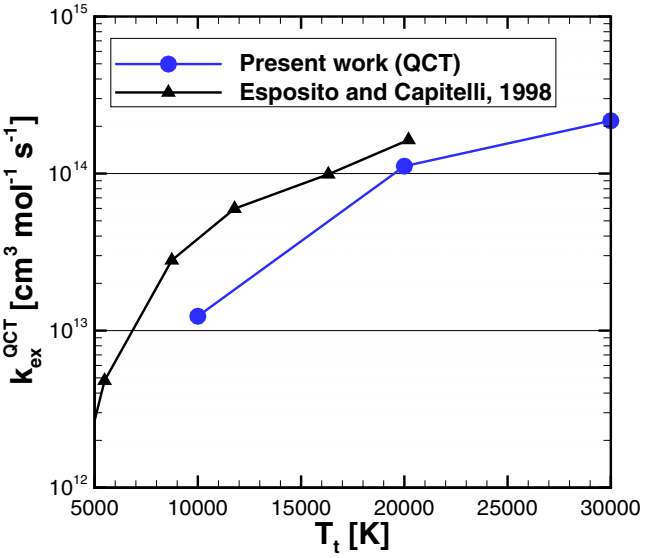

FIG. 11. Comparison between QCT results obtained in this study and the QCT results of Esposito and Capitelli [13].

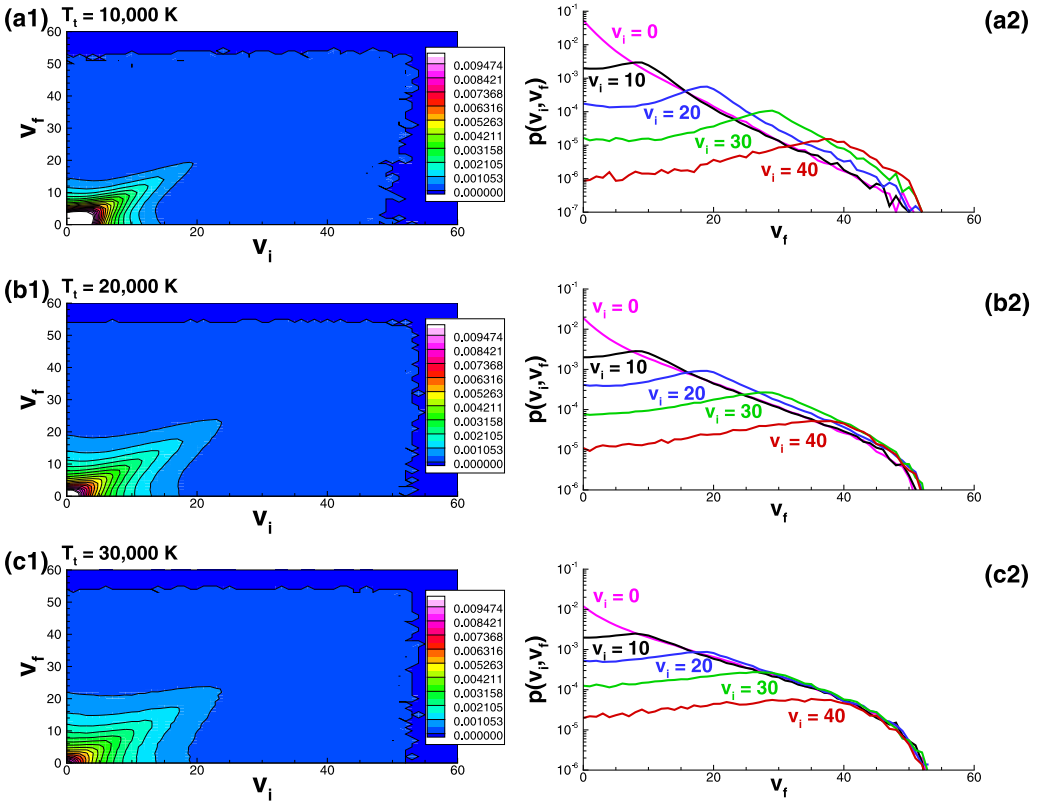

FIG. 12. (a) Probability map for exchange reactions where the reactant molecule occupies a vibrational state v_i and the product molecule occupies a vibrational state v_f. (b) Selected cuts at $v_i = \{0,10,20,30,40\}$.

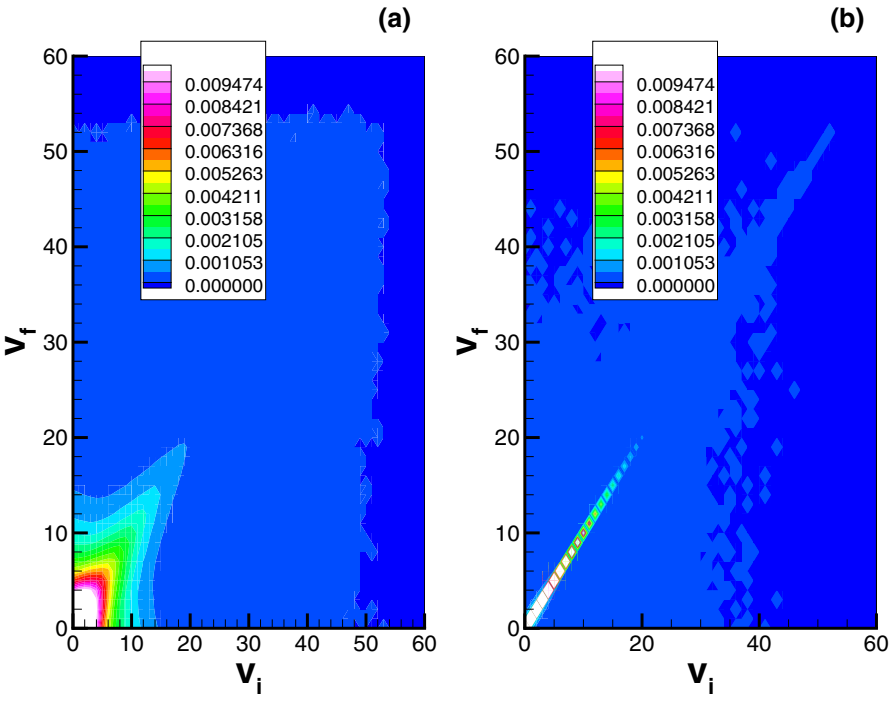

FIG. 13. Probability map, at $T_t = 10\,000$ K, for (a) $N + N_2$ exchange reactions and (b) nonreactive $N + N_2$ collisions where the reactant molecule occupies a vibrational state v_i and the product molecule occupies a vibrational state v_f.

single- and multiquantum jumps becomes extremely small for $|v_f - v_i| \gg 0$, as also previously observed for $N_2 + N_2$ interactions [3].

Finally, we extracted several *cuts* from $p(v_i, v_f)$ for nonreactive $N + N_2$ [Fig. 13(b)] collisions and from $p(v_i, v_f)$ (not shown) for nonreactive $N_2 + N_2$ collisions. To account for the relative importance of populations of molecules in each v_i state, we plotted $p(v_i, v_f)p(v_i)$, where $p(v_i)$ is the QSS distribution, as shown in Fig. 9. Compared to the corresponding results for exchange reactions, the distributions $p(\{0,10,20\}, v_f)p(v_i)$ (in Fig. 14) are narrowly peaked around v_i, particularly for $N_2 + N_2$ interactions. Because the largest fraction of molecules is in $v_i = 0$, a transition, for example, from $v_i = 0$ to $v_f = 10$ is about a thousand times more likely with an exchange process than a nonreactive inelastic collision between two molecules. Finally, we note that transitions from high-v states to low-v states via exchange reactions (similar to nonreactive inelastic collisions) become more rare as v_i is increased, due to the fast drop of $p(v_i)$. In summary, these simulations show that multiquantum transitions out of the ground state are greatly facilitated by exchange events in $N + N_2$ interactions and, given the overwhelmingly large fraction of molecules occupying $v = 0$, particularly at 10 000 K, this might indeed be the first-order effect on the reduction of τ_{N_3} compared to τ_{N_4}.

E. Comparison to Park's model

Figure 15 shows a comparison between composition histories obtained from DMS and from Park's two-temperature model [6] with relaxation times obtained from the Millikan-White correlation, for an isothermal system initially containing only nitrogen molecules ($\rho_{N_2}/\rho_{tot} = 1$) in thermal equilibrium ($T_v(0) = T_t$). At 10 000 K [Fig. 15(a)] and 20 000 K [Fig. 15(b)], Park's model predicts a much faster dissociation process than that obtained with DMS, whereas only a small difference is seen at 30 000 K [Fig. 15(c)]. Qualitatively, the Park and DMS predictions become closer as T_t is increased.

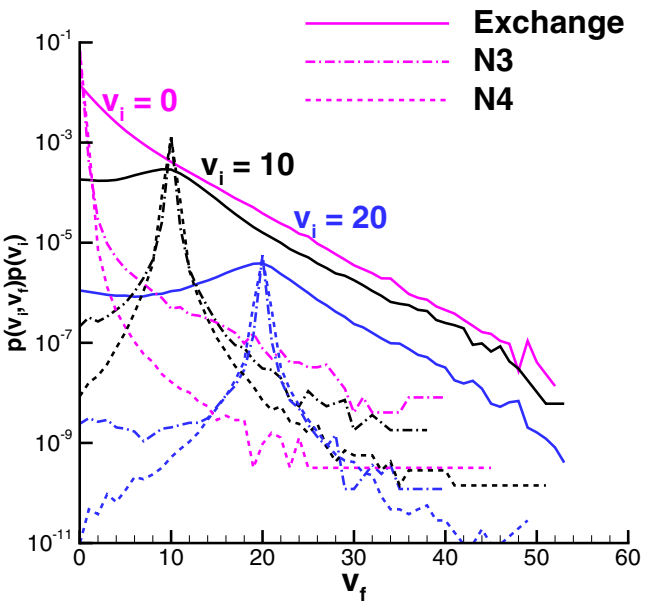

FIG. 14. Distribution functions for exchange, (nonreactive) $N + N_2$, and (nonreactive) $N_2 + N_2$ collisions, where the reactant molecule occupies a vibrational state $v_i = \{0, 10, 20\}$ and the product molecule occupies a vibrational state v_f. The translational temperature is 10 000 K.

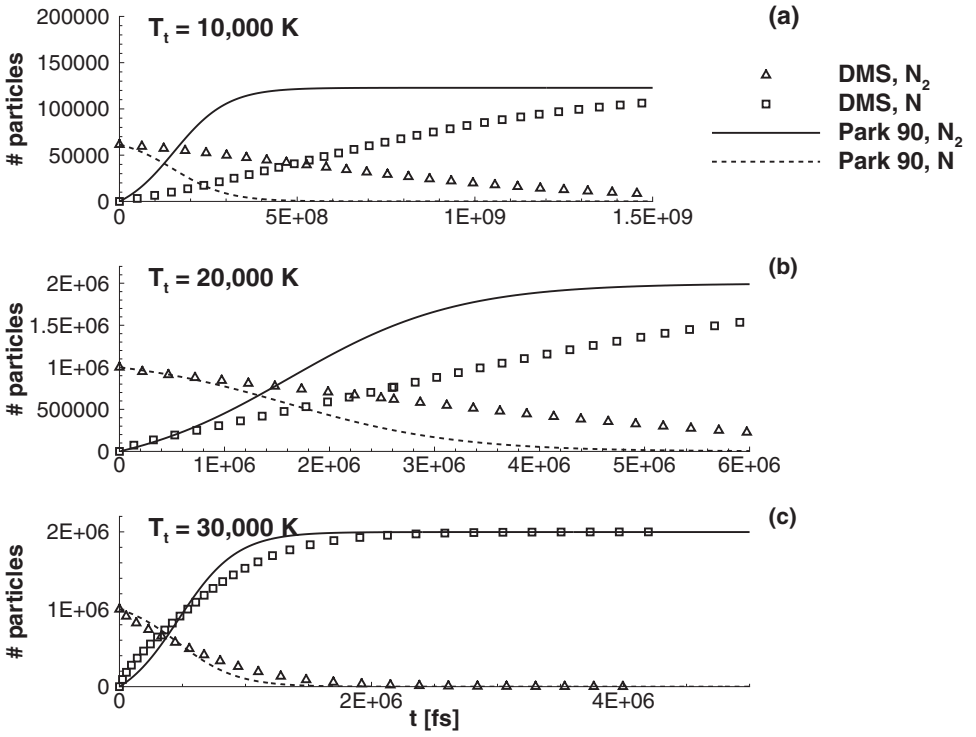

FIG. 15. Comparison between DMS calculations (symbols) and Park's two-temperature model [6] predictions (lines) for isothermal relaxations from thermal equilibrium ($T_v = T_t$) initial conditions.

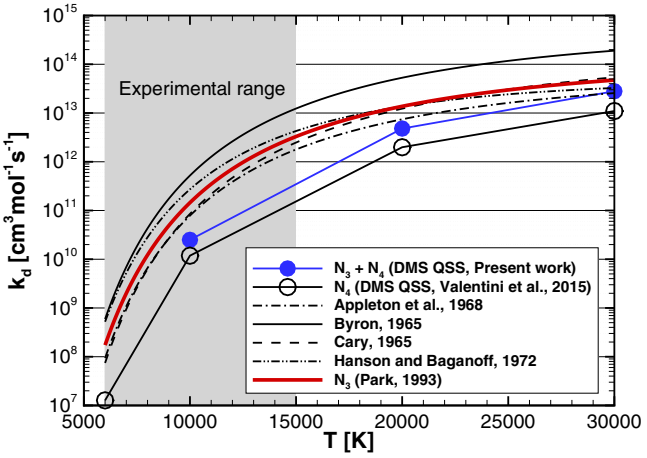

FIG. 16. Comparison between DMS calculations (symbols), experimental data (and their high-temperature extrapolations), and Park's model [6] for N_3 dissociation rates (lines).

This trend is explained by inspection of Fig. 16, where it can be seen that all experimental data (except Byron's [33]) approach the DMS rates as temperature is increased. As shown in Fig. 16, Park's rates, which are an overall fit of those data, closely approach the DMS rate coefficient at 30 000 K.

Finally, we point out that there is general consensus [33–36] that $k^{\mathrm{DMS}}_{d,\mathrm{N_4}} < k^{\mathrm{DMS}}_{d,\mathrm{N_3+N_4}}$ (although the magnitude of such a difference varies greatly among the various experimental results), and experimentalists have attributed this behavior to the fact that nitrogen atoms are more efficient than nitrogen molecules at dissociating other nitrogen molecules. The DMS results have also shown this trend ($k^{\mathrm{DMS}}_{d,\mathrm{N_3+N_4}} \simeq (2-3)k^{\mathrm{DMS}}_{d,\mathrm{N_4}}$), but because of an indirect mechanism: In fact, atom-diatom inelastic collisions and atom-diatom exchange processes reduce the overall vibrational relaxation time, as shown in Fig. 4. This, in turn, speeds up the replenishment of high-v states (Fig. 9). The consequence of a reduction in the vibrational relaxation times is that QSS vibrational energy distributions for systems in which *both* $\mathrm{N}+\mathrm{N_2}$ and $\mathrm{N_2}+\mathrm{N_2}$ collisions occur exhibit higher populations of high-v states (Fig. 9) than in systems where $\mathrm{N_2}+\mathrm{N_2}$ *only* collisions occur. Hence, because more molecules now occupy high-v states, dissociation proceeds at a rate closer to the equilibrium rate (Fig. 8).

IV. CONCLUSIONS

In this article, we have presented a molecular-level investigation of dissociation in nitrogen at high temperature. For the first time in literature, *both* $\mathrm{N}+\mathrm{N_2}$ and $\mathrm{N_2}+\mathrm{N_2}$ processes are simulated as they concurrently take place in an evolving nonequilibrium zero-dimensional gas system. The computational technique (DMS) solely relies on a single *ab initio* PES [26] that accurately fits the extensive database of quantum mechanical calculations for high-energy $\mathrm{N}+\mathrm{N_2}$ and $\mathrm{N_2}+\mathrm{N_2}$ interactions of Paukku and coworkers [18].

In the range of temperatures considered, equilibrium QCT calculations have revealed that, on average, collisions between a nitrogen atom and a nitrogen molecule are only slightly more likely to result in the dissociation of the N_2 molecule as collisions between two nitrogen molecules.

The DMS (nonequilibrium) simulations indicate, however, that the presence of atomic nitrogen significantly affects the dissociation rate of molecular nitrogen, but indirectly. We find that atomic nitrogen causes an important reduction of the vibrational relaxation time of N_2, by almost one order of magnitude, as shown in Fig. 5. This, in turn, speeds up the replenishment of high-v states with a consequent reduction of the degree of depletion of high vibrational energy states (Fig. 9) compared to N_4 systems (i.e., where $\mathrm{N_2}+\mathrm{N_2}$ only collisions take place). Because high-v states dissociate more

readily, this results in dissociation rates (Fig. 8) that are about 2–3 faster than the corresponding rates for N_4 systems. The nonequilibrium reaction rates presented are specific to the QSS regime where high-v state populations are depleted. Although accessible by DMS [37], dissociation during rovibrational excitation was not studied in this article. Prior master equation research [8] has shown that, in some cases, significant dissociation can occur during the transient rovibrational excitation phase before QSS.

As illustrated in Fig. 10, the analysis of normalized distributions of precollision states for dissociated N_2 molecules reveals a strong bias to dissociation from high-vibrational-energy states, particularly at low temperature (10 000 K). At high temperatures (20 000 K and 30 000 K), preferential dissociation, although still significant, is less marked than at low temperature, and nitrogen molecules dissociate more uniformly across the whole vibrational energy ladder, due to the increased availability of collisional translation energy in each interaction. This behavior is qualitatively similar to what was found for N_4 systems using the same numerical techniques and PES [3].

Arguably, the main microscopic difference between N_3 and N_4 systems is related to exchange processes. We found that an exchange event is very likely to occur whenever a nitrogen atom and a nitrogen molecule collide. Furthermore, the ratio of the QCT exchange rate constant to the QCT dissociation rate constant (Table I) increases as the translational temperature is reduced.

Statistical distributions collected on such transitions are *diffuse*, thus indicating a rather effective mechanism of scrambling the internal energy states, particularly in facilitating transitions out of the vibrational ground state. Because the vast majority of molecules occupy $v_i = 0$, we think that this is the first-order effect that affects the vibrational relaxation time. On the contrary, in nonreactive inelastic collisions, the probability of single- and multiquantum jumps becomes extremely small for $|v_f - v_i| \gg 0$, as shown in Figs. 13 and 14 and previously reported by us for $N_2 + N_2$ interactions [3].

Finally, discrepancies were found between Park's two-temperature model [6] predictions and the DMS results, particularly at the lowest temperature considered here (10 000 K). Specifically, composition histories computed using Park's rates show a faster dissociation process than the DMS calculations. At 30 000 K, however, where Park's and DMS rates nearly coincide, composition histories become close.

In conclusion, a number of fundamental mechanisms that characterize the dissociation of N_2 under nonequilibrium conditions due to concurrent $N + N_2$ and $N_2 + N_2$ interactions have been identified with QCT and DMS calculations based on the same *ab initio* PES. The comparison with Park's model shows that the DMS technique is able to produce results, both macroscopic (e.g., energy and composition histories) and microscopic (e.g., distributions of reactive and nonreactive events), that can be used to develop and test simplified models for use in CFD or DSMC.

ACKNOWLEDGMENTS

The research is supported by Air Force Office of Scientific Research (AFOSR) under Grants No. FA9550-10-1-0563 and No. FA9550-16-1-0161. Partial support for J. D. Bender in this work was provided by the US Department of Energy Computational Science Graduate Fellowship (DOE CSGF) under Grant No. DE-FG02-97ER25308. The views and conclusions contained herein are those of the authors and should not be interpreted as necessarily representing the official policies or endorsements, either expressed or implied, of the AFOSR or the US government. We would like to thank Ross Chaudhry for his help with Park's model.

[1] M. Cacciatore, A. Kurnosov, and A. Napartovich, Vibrational energy transfer in N_2-N_2 collisions: A new semiclassical study, J. Chem. Phys. **123**, 174315 (2005).

[2] V. Guerra and J. Loureiro, Non-equilibrium coupled kinetics in stationary N_2-O_2 discharges, J. Phys. D Appl. Phys. **28**, 1903 (1995).
[3] P. Valentini, T. E. Schwartzentruber, J. D. Bender, I. Nompelis, and G. V. Candler, Direct molecular simulation of nitrogen dissociation based on an *ab initio* potential energy surface, Phys. Fluids **27**, 086102 (2015).
[4] C. Park, Assessment of a two-temperature kinetic model for dissociating and weakly ionizing nitrogen, J. Thermophys. Heat Tr. **2**, 8 (1988).
[5] C. Park, Assessment of two-temperature kinetic model for ionizing air, J. Thermophys. Heat Tr. **3**, 233 (1989).
[6] C. Park, Review of chemical-kinetic problems of future NASA missions, I: Earth entries, J. Thermophys. Heat Tr. **7**, 385 (1993).
[7] M. Lino da Silva, V. Guerra, and J. Loureiro, Two-temperature models for nitrogen dissociation, Chem. Phys. **342**, 275 (2007).
[8] M. Panesi, R. L. Jaffe, D. W. Schwenke, and T. E. Magin, Rovibrational internal energy transfer and dissociation of $N_2(^1\sum_g^+)$-$N(^4S_u)$ system in hypersonic flows, J. Chem. Phys. **138**, 044312 (2013).
[9] J. G. Kim and I. D. Boyd, State-resolved master equation analysis of thermochemical nonequilibrium of nitrogen, Chem. Phys. **415**, 237 (2013).
[10] P. Valentini, P. Norman, C. Zhang, and T. E. Schwartzentruber, Rovibrational coupling in molecular nitrogen at high temperature: An atomic-level study, Phys. Fluids **26**, 056103 (2014).
[11] F. Esposito, I. Armenise, and M. Capitelli, N-N_2 state to state vibrational-relaxation and dissociation rates based on quasiclassical calculations, Chem. Phys. **331**, 1 (2006).
[12] F. Esposito, M. Capitelli, and C. Gorse, Quasi-classical dynamics and vibrational kinetics of $N + N_2(v)$ system, Chem. Phys. **257**, 193 (2000).
[13] F. Esposito and M. Capitelli, Quasiclassical molecular dynamic calculations of vibrationally and rotationally state selected dissociation cross-sections: $N + N_2(v,j) \rightarrow 3N$, Chem. Phys. Lett. **302**, 49 (1999).
[14] G. D. Billing and E. R. Fisher, VV and VT rate coefficients in N_2 by a quantum-classical model, Chem. Phys. **43**, 395 (1979).
[15] A. Lagana, E. Garcia, and L. Ciccarelli, Deactivation of vibrationally excited nitrogen molecules by collision with nitrogen atoms, J. Phys. Chem. **91**, 312 (1987).
[16] A. Lagana and E. Garcia, Temperature dependence of nitrogen atom-molecule rate coefficients, J. Phys. Chem. **98**, 502 (1994).
[17] C. Zhang and T. E. Schwartzentruber, Consistent implementation of state-to-state collision models for direct simulation Monte Carlo, in *52nd Aerospace Sciences Meeting, AIAA SciTech, National Harbor, Maryland*, AIAA Paper 2014-0866 (AIAA, Reston, 2014).
[18] Y. Paukku, Y. R. Ke, Z. Varga, and D. G. Truhlar, Global *ab initio* ground-state potential energy surface of N_4, J. Chem. Phys. **139**, 044309 (2013).
[19] J. D. Bender, S. Doraiswamy, D. G. Truhlar, and G. V. Candler, Potential energy surface fitting by a statistically localized, permutationally invariant, local interpolating moving least squares method for the many-body potential: Method and application to N_4, J. Chem. Phys. **140**, 054302 (2014).
[20] D. G. Truhlar and J. T. Muckerman, *Atom-Molecule Collision Theory: A Guide for the Experimentalist* (Plenum, New York, 1979), p. 5.
[21] K. Koura, Monte Carlo direct simulation of rotational relaxation of diatomic molecules using classical trajectory calculations: Nitrogen shock wave, Phys. Fluids **9**, 3543 (1997).
[22] K. Koura, Monte Carlo direct simulation of rotational relaxation of nitrogen through high total temperature shock waves using classical trajectory calculations, Phys. Fluids **10**, 2689 (1998).
[23] H. Matsumoto and K. Koura, Comparison of velocity distribution functions in argon shock wave between experiments and Monte Carlo calculations for Lennard-Jones potential, Phys. Fluids **3**, 3038 (1991).
[24] P. Norman, P. Valentini, and T. E. Schwartzentruber, GPU-accelerated classical trajectory calculation direct simulation Monte Carlo applied to shock waves, J. Comput. Phys. **247**, 153 (2013).

[25] I. Nompelis and T. E. Schwartzentruber, Strategies for parallelization of the DSMC method, in *51st AIAA Aerospace Sciences Meeting, Grapevine, TX*, AIAA Paper 2013-1204 (AIAA, Reston, 2013).
[26] J. D. Bender, P. Valentini, I. Nompelis, Y. Paukku, Z. Varga, D. G. Truhlar, T. E. Schwartzentruber, and G. V. Candler, An improved potential energy surface and multi-temperature quasiclassical trajectory calculations of $N_2 + N_2$ dissociation reactions, J. Chem. Phys. **143**, 054304 (2015).
[27] D. Frenkel and B. Smit, *Understanding Molecular Simulation* (Academic Press, San Diego, 2002).
[28] G. A. Bird, *Molecular Gas Dynamics and the Direct Simulation of Gas Flows* (Clarendon, Oxford, UK, 1994).
[29] R. C. Millikan and D. R. White, Systematics of vibrational relaxation, J. Chem. Phys. **39**, 3209 (1963).
[30] I. D. Boyd and E. Josyula, State resolved vibrational relaxation modeling for strongly nonequilibrium flows, Phys. Fluids **23**, 057101 (2011).
[31] C. Park, Rotational relaxation of N_2 behind a strong shock wave, J. Thermophys. Heat Tr. **18**, 527 (2004).
[32] M. Karplus, R. N. Porter, and R. D. Sharma, Exchange reactions with activation energy. I. Simple barrier potential for (H, H_2), J. Chem. Phys. **43**, 3259 (1965).
[33] S. Byron, Shock-tube measurement of the rate of dissociation of nitrogen, J. Chem. Phys. **44**, 1378 (1966).
[34] B. Cary, Shock-tube study of the termal dissociation of nitrogen, Phys. Fluids **8**, 26 (1965).
[35] J. P. Appleton, M. Steinberg, and D. J. Liquornik, Shock-tube study of nitrogen dissociation using vacuum-ultraviolet light absorption, J. Chem. Phys. **48**, 599 (1968).
[36] R. K. Hanson and D. Baganoff, Shock-tube study of nitrogen dissociation rates using pressure measurements, AIAA J. **10**, 211 (1972).
[37] N. Singh, P. Valentini, and T. E. Schwartzentruber, A coupled vibration-dissociation model for nitrogen from direct molecular simulation, in *46th AIAA Thermophysics Conference, AIAA Aviation, Washington D.C.*, AIAA Paper 2016-4318 (AIAA, Reston, 2016).